Goal-Oriented Resource Allocation and Scheduling for Integrated Sensing and Communications

Tran Trong Duy, Maxime Ferreira da Costa, Salah Eddine Elayoubi, Nguyen Linh Trung

Goal-Oriented Resource Allocation and Scheduling for Integrated Sensing and Communications

Tran Trong Duy*†, Maxime Ferreira Da Costa*, Salah Eddine Elayoubi*, Nguyen Linh Trung†
*Laboratory of Signals and Systems, CentraleSupélec, Université Paris-Saclay, CNRS, Gif-sur-Yvette, France
†University of Engineering and Technology, Vietnam National University, Hanoi, Vietnam

***Abstract*—This paper proposes a goal-oriented design framework for Integrated Sensing and Communications (ISAC) at the network layer. Devices equipped with dual-functional radar and communication (DFRC) transceivers that jointly perform a sensing task and carry data traffic are considered. The goal of the sensing application is to maximize the classification accuracy, while the network aims to preserve throughput for the enhanced Mobile Broadband (eMBB) service and to respect energy constraints. A cross-layer optimization problem that adapts the lower layer parameters (sensing power and scheduling policy) for maximizing the classification accuracy, while respecting constraints related to the available resources (eMBB throughput, device's maximal power, and total energy), is formulated. A tractable relaxation of the problem is proposed, yielding an approximate optimal policy that is computable by solving successive convex optimization problems. Our numerical experiments, conducted both on a synthetic Gaussian mixture dataset and on a radar simulation dataset, show the superiority of our goal-oriented scheme policy to classical ISAC schemes.**

***Index Terms*—ISAC, goal-oriented communications.**

I. Introduction

Integrated Sensing and Communications (ISAC) integrates radar sensing and wireless communications into the same hardware and uses the RF signals for sensing [1]. ISAC has been extensively studied in the past few years and is considered an essential enabler for 6G networks [2]. Fundamental performance limits have been studied from an information-theoretical point of view in [3]. From the physical layer perspective, the tradeoff between radar metrics (detection probability, resolution, etc.) and the communication link capacity has been studied in [4]–[6]. However, ISAC is not restricted to the physical layer, and it includes the broader concept of the cross-layer design of 6G networks for conveying sensing information in an optimal way [1], [7]–[10]. The sensory data have been exploited in [7] for training a deep neural network (DNN) for recognizing human activities. Multi-view sensing data have been used in [8] for extracting features, and the communication link is used for conveying them to a centralized edge server that conducts the model inference. A distributed source estimation problem is considered in [9], where sensors have partial information about the source and use the communication channel for sharing data and performing estimation.

While the majority of ISAC literature focuses on the performance tradeoffs between sensing and communications, there is still a need for a global design framework that considers the networking and sensing constraints and goals. We argue in this paper that goal-oriented communication is an adequate paradigm in this context. Goal-oriented communications have emerged as a novel paradigm in wireless networks, and are expected to be an integral part of 6G systems [11], [12]. Goal relates to the performance of a specific application, rather than classical telecommunication metrics such as the Quality of Service (QoS) (throughput, delay, etc.). In other words, goal-oriented communications aim to maximize the impact of the received bits for a custom goal intended by the transmitter and the receiver [11]. It is sometimes called task-oriented, as in [13], and has been identified as an enabler for sustainable networking, as only the necessary amount of data for achieving the goal is transmitted [14].

We consider in this paper an ISAC system designed under a goal related to the sensing accuracy, measured in terms of the discriminant gain [15]. We also integrate the classical communication requirement, measured in terms of data rate for the enhanced Mobile Broadband (eMBB) [16]. Our goal-oriented design leverages two factors: sensing power and scheduling policy. The former is a classical optimization lever for ISAC, while the current paper is the first to consider scheduling and resource allocation as a part of the ISAC system design. We formulate an optimization problem that maximizes the sensing accuracy under constraints on devices' powers, eMBB data rate, and total energy. The problem solution provides both the optimal selection of devices to be sampled and their corresponding sensing powers.

The original contributions of the paper are as follows:

- We propose in Section II a novel goal-oriented system design framework for ISAC, that considers both the physical layer and network aspects (scheduling and resource allocation), and that integrates a global vision of the system with the presence of multiple devices and eMBB service. This extends from the state of the art [8] which only focuses on the physical layer. Our cross-layer scheme thus integrates the physical, MAC (Medium Access Control), and application layers.
- We formulate in Section III a constrained optimization problem that ensures scalability by selecting the optimal subset of sensors to query within the available resources, while maximizing the application goal.
- Numerical results show in Section IV that the proposed goal-oriented scheme is able to preserve the sensing accuracy under high-level guarantees on eMBB performance.

This work has been partially supported by the Sustainable 6G chair, funded by Orange and held by CentraleSupélec.

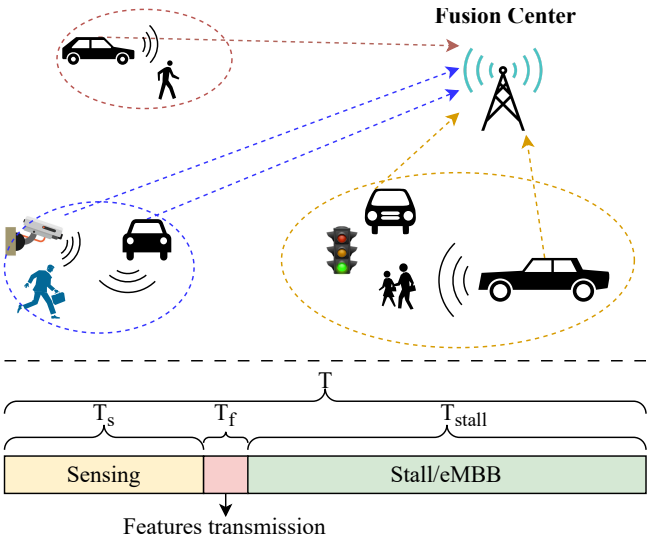

Figure 1: Network sensing model

II. System Model

A. Distributed Sensing Model

We consider a scenario where K devices sense an environment under the query of a fusion center. The fusion center selects a policy that dictates the expected probability of selecting a device for the sensing task and the power a device must allocate to sensing. Then, at the beginning of a monitoring cycle, the devices that are selected for sensing according to the scheduling policy dedicate a share of power to gather environmental data (*e.g., radar sensing, video monitoring*), and extract features out of this recording. At the end of the monitoring cycle, the features are sent to the fusion center, which performs a classification task by harnessing the gathered features.

In this paper, we assume the goal sought by the fusion center is to classify targets in the environment. To that end, the smart devices employ dual-functional radar and communication (DFRC) transceivers [17] and only switch to sensing mode when scheduled. A sensing cycle consists of three stages: sensing, feature transmission, and stall. In the sensing stage, the scheduled devices use frequency-modulated continuous-wave (FMCW) radar waveforms to sense the environment. Then, they extract features locally, transmit them to the fusion center, and finally stall until the beginning of the next sensing cycle. During this stalling period, their transceivers can be used for classical communication. When a device is not scheduled for sensing by the fusion center during the cycle, it uses its transceivers for classical communications for the whole cycle. The overall setup is illustrated in Figure 1.

B. Sensing Task and Network Classification Metric

Let T_s, T_f, and T_{stall} denote the duration of the sensing time, the feature transmission time, and the stalling time (Figure 1), respectively. The duration of the sensing cycle T is thus given by $T = T_s + T_f + T_{stall}$. After sensing, the k-th device extracts a feature vector $\boldsymbol{x}_k \in \mathbb{C}^{N_k}$ which we model as a random vector whose probability distribution depends on the state of the environment that we want to estimate. We write $p_{k,\ell} = \mathbb{P}(\boldsymbol{x}_k|H_\ell)$ the conditional probability distribution of $\boldsymbol{x}_k$ given the hypothesis H_ℓ that the target belongs to the ℓ-th class, $\ell \in \{1, 2, \dots, L\}$. For statistical and optimization convenience, we focus on the case where the conditional distributions of the classes are Gaussian, that is

$$p_{k,\ell} = \mathcal{N}\left(\boldsymbol{\mu}_{k,\ell}, \boldsymbol{\Sigma}_k + \frac{\sigma_r^2}{P_{s,k}} \boldsymbol{I}_{N_k}\right) \tag{1}$$

where $\boldsymbol{\mu}_{k,\ell} = \{\mu_{n_k,\ell}\}_{1_k}^{N_k}$ is the mean value of $\boldsymbol{x}_k$ under H_ℓ. The residual variance of $\boldsymbol{x}_k$ and the noise variance are denoted $\boldsymbol{\Sigma}_k = diag(\sigma_{1_k}, \cdots, \sigma_{n_k})$ and σ_r^2, respectively, which are assumed to be independent of ℓ, while $P_{s,k}$ is the power allocated by the k-th device to sensing. In our model (1), the variance of $p_{k,\ell}$ decreases with $P_{s,k}$, and converges to the residual variance $\boldsymbol{\Sigma}_k$ in the asymptotic $P_{s,k} \to \infty$.

We assess the goodness of the classification task in terms of its *discriminant gain* [15], which measures the discernibility between the classes. At the k-th sensor, the pairwise discriminant gain between two hypothesis (or classes) H_ℓ and $H_{\ell'}$ is defined as the symmetric Kullback-Leibler (KL) divergence between the conditional probability density $p_{k,\ell}$ and $p_{k,\ell'}$. That is, under the Gaussian assumption (1):

$$\begin{aligned} G_k^{(\ell,\ell')}(P_{s,k}) &\triangleq \mathrm{D_{KL}}\left(p_{k,\ell} \,\|\, p_{k,\ell'}\right) + \mathrm{D_{KL}}\left(p_{k,\ell'} \,\|\, p_{k,\ell}\right) \\ &= \sum_{n_k=1}^{N_k} \frac{(\mu_{n_k,\ell} - \mu_{n_k,\ell'})^2}{\sigma_{n_k}^2 + \sigma_r^2/P_{s,k}}. \end{aligned} \tag{2}$$

When the number of classes is greater than two, the discriminant gain is defined as the smallest discriminant gain between any two classes

$$\overline{G}_k(P_{s,k}) = \min_{\ell \neq \ell'} G_k^{(\ell,\ell')}(P_{s,k}), \tag{3}$$

reflecting the least distinguishable pair of classes at the k-th sensor. The metric (2) is theoretically grounded since the KL divergence provides a lower bound of the error exponent of the probability of error of the optimal Hoeffding test [18].

In our distributed sensing model, the fusion center dictates a policy $\{\boldsymbol{\pi} = [\pi_1, \cdots, \pi_K], \boldsymbol{P}_s = [P_{s,1}, \dots, P_{s,K}]\}$, where π_k controls the fraction of time that the k-th device in the network have to allocate to the common sensing task with sensing power $P_{s,k}$. The *network discriminant gain* under a policy $\{\boldsymbol{\pi}, \boldsymbol{P}_s\}$ is defined at the fusion center as the linear combination of the sensor's discriminant gain, weighted by the scheduling policy $\boldsymbol{\pi}$, that is

$$G(\boldsymbol{\pi}, \boldsymbol{P}_s) = \sum_{k=1}^{K} \pi_k \overline{G}_k(P_{s,k}). \tag{4}$$

Under the additional assumption that the conditional distribution $\{p_{1,\ell}, \dots, p_{K,\ell}\}$ are jointly independent for $\ell \in \{1, \dots, L\}$, the network discriminant gain (4) also indicate a lower bound on the error exponent of the classification task

based on the merged data from the K sensors at the fusion center.

While the application goal is usually expressed in terms of the realized accuracy of the fusion center's classification, the network discriminant gain (4) provides a good proxy for it. In Section IV, a numerical experiment will showcase that policies achieving higher network discriminant gain also achieve superior classification accuracy.

III. Goal-Oriented System Design

A. Problem Formulation

The sensing performance model described above supposes the collaboration of K devices, with device k extracting N_k features, leading to the total discriminant gain of Equation (4). This gain depends on both physical and network layer parameters:

- *At the physical level,* in sensing application perspective, quality of the observation associated with each of the devices encompassed in the probability distribution $p_{k,\ell}$ in Equation (1) affects the classification performance. While, the distribution mean $\boldsymbol{\mu}_{k,\ell}$ and residual variance $\boldsymbol{\Sigma}_{k,\ell}$ are imposed by the sensing environment (*e.g.* the device processing capacity, the physical location of the device, ...) and cannot be controlled by the system, the sensing power $P_{s,k}$ is an optimization lever that influences the application performance.
- *At the network level,* because of quality of service and resource constraints, not all devices can be queried in a cycle. An important optimization lever is the scheduling policy selected by the fusion center, which selects the subset of devices to query at each cycle. The scheduling probability $\boldsymbol{\pi}$ integrates the expected contribution of the device to the application goal, such as in Equation (2), but also its radio conditions, which define the cost for sending its data on the radio interface. We denote by e_k the spectral efficiency of the k-th device, which can be computed from the signal to Interference and Noise ratio (SINR) as $e_k = f(\text{SINR}_k)$ via the modified Shannon formula as in [19], or using simulation-based link level curves as in [20].

Our goal-oriented design framework aims at maximizing the application goal, modeled as the network discriminant gain (4) by acting on both the sensing power of the DFRC transceiver $\boldsymbol{P}_r = [P_{s,1}, \dots, P_{s,K}] \in \mathbb{R}^{+K}$ and the scheduling policy of the network $\boldsymbol{\pi} \in [0,1]^K$. Hence, our application objective is

$$\underset{\boldsymbol{\pi}\in[0,1]^K, \boldsymbol{P}_s\in\mathbb{R}^{+K}}{\text{maximize}} \quad G(\boldsymbol{\pi}, \boldsymbol{P}_s). \tag{5}$$

This objective (5) is maximized under different constraints reflecting the limited sensing capabilities of the devices, the network resources, the service requirements of the data network, and the total energy. The modeling constraints are detailed in the following.

1) *Device power constraint:* The sensing power is naturally limited by hardware specification. Additionally, depending on the operating mode or battery level, the device can set a logical limit on the sensing power,

$$P_{s,k} \leq P_{\max,k}, \quad k \in \{1, \cdots, K\}. \tag{C1}$$

2) *eMBB data rate constraint:* Assuming that the base station deploys a fair bandwidth-sharing strategy for regular data, the average rates of the three stages are as follows. During the stall stage, the k-device can transmit at the rate

$$r_k^{stall} = \frac{e_k B}{K},$$

where e_k is the spectral efficiency of the k-th device and B is the communication bandwidth. During the sensing stage, the k-device can only transmit if it has been scheduled for sensing by the fusion center. Hence, the k-th device transmits eMBB data with a probability of $1 - \pi_k$. Assuming the scheduling policies are independent between devices, the k-th device's average transmission rate during the sensing stage is

$$r_k^s = (1 - \pi_k)\mathbb{E}\left[\frac{e_k B}{1 + m_k}\right],$$

where m_k is the number of other devices sending eMBB data simultaneously with the k-th device, $P[m_k = m] = \sum_{A\in F_m} \prod_{i\in A}(1-\pi_i) \prod_{j\in A^c} \pi_j$, F_m is the set of all subsets of m integers selecting from $\{1, \dots, K\} \setminus \{k\}$, and the complement $A^c = \{1, \dots, K\} \setminus \{k\} \setminus A$. Furthermore, during the feature transmission stage, the devices report the acquired features to the fusion center. Consequently, there is no eMBB transmission, that is $r_k^f = 0$. Hence, the final average eMBB rate for device k is

$$\begin{aligned} r_k^{avg} &= \frac{1}{T}\left(T_{stall} r_k^{stall} + T_s r_k^s + T_f r_k^f\right) \\ &= \frac{e_k B}{T}\left(\frac{T_{stall}}{K} + T_s(1-\pi_k)\mathbb{E}\left[\frac{1}{1+m_k}\right]\right). \end{aligned} \tag{6}$$

The base station should guarantee a minimum eMBB rate for each device depending on its radio conditions:

$$r_k^{avg} \geq r_k^{\min}, \quad k \in \{1, \cdots, K\}. \tag{C2}$$

The guarantee levels $r_k^{\min}$ in constraint (C2) can be device-dependent, as devices with less favorable radio conditions would consume a larger amount of resources if guaranteed at the same throughput as devices with a large SINR. However, our model remains general and allows an arbitrary guarantee policy $[r_1^{\min}, \dots, r_K^{\min}]$. A selection method for the guarantee policy is proposed in Section IV.

3) *Total energy constraint:* To better control the energy consumption of the system, the total energy for the sensing service is bounded by an energy budget E, yielding

$$\sum_{k=1}^{K} \left(P_{s,k} T_s + P_{f,k} T_f\right) \pi_k \leq E, \tag{C3}$$

where $P_{f,k}$ is the feature transmission power of the k-th device.

With the above constraints, the *optimal policy* for our goal-oriented scheduling problem reads

$$\begin{aligned} \underset{\boldsymbol{\pi}, \boldsymbol{P}_s}{\text{maximize}} \quad & G(\boldsymbol{\pi}, \boldsymbol{P}_s) \\ \text{subject to} \quad & \pi_k \in [0,1], \quad k \in \{1, \dots, K\} \\ & P_{s,k} \in \mathbb{R}^+, \quad k \in \{1, \dots, K\} \\ & \text{(C1) and (C2) and (C3).} \end{aligned} \tag{P0}$$

B. Policy Derivation

The optimal policy definition (P0) is elusive as the program (P0) is computationally intractable due to the combinatorial aspect of the objective function (4) and the non-convex constraints. In this section, we construct an *approximate* optimal policy by relaxing the cost and constraints of (P0) into reasonable convex surrogates which are well-behaved and tractable for optimization purposes.

First, the ideal discriminant gain (3) suggests maximizing the sum of the minimal discriminant gains for all devices. However, this is not tractable. Instead of (3), we propose maximizing for each device the sum of discriminant gains:

$$\widehat{G}_k(P_{s,k}) = \sum_{l=1}^{L} \sum_{l'>l} \sum_{n_k=1}^{N_k} \frac{(\mu_{n_k,\ell} - \mu_{n_k,\ell'})^2}{\sigma_{n_k}^2 + \sigma_r^2/P_{s,k}},$$

which is a concave function of $P_{s,k}$. In the view of (4), the *approximate network discriminant gain* is defined as

$$\widehat{G}(\boldsymbol{\pi}, \boldsymbol{P}_s) = \sum_{k=1}^{K} \pi_k \widehat{G}_k(P_{s,k}), \tag{7}$$

Secondly, no closed-form formula is available for the expectation in (6). Hence, we approximate (6) by its first-order Taylor expansion around $\mathbb{E}[m_k] = K - 1 - \sum_{i\neq k}^{K} \pi_i$ yielding

$$r_k^{avg} \approx \frac{e_k B}{T} \left(\frac{T_{stall}}{K} + T_s \frac{1-\pi_k}{K - \sum_{i\neq k}^{K} \pi_i} \right), \tag{8}$$

for all $k \in \{1, \cdots, K\}$. With Equation (8), the linearization of the constraint (C2) is

$$\pi_k - \left(\frac{r_k^{\min} T}{e_k B T_s} - \frac{T_{stall}}{K T_s} \right) \sum_{i\neq k}^{K} \pi_i \leq K \left(\frac{T_{stall}}{K T_s} - \frac{r_k^{\min} T}{e_k B T_s} \right) + 1. \tag{$\widetilde{\text{C2}}$}$$

Lastly, the constraint (C3) is bilinear, and all the optimization variables $\boldsymbol{\pi}$ and $\boldsymbol{P}_s$ are bounded. Hence, the McCormick envelopes [21] can be utilized to relax (C3) into the set of linear constraints as follows:

$$\sum_{k=1}^{K} \left(P_{max,k} T_s + P_{f,k} T_f \right) \pi_k \leq E \tag{$\widetilde{\text{C3.a}}$}$$

$$\sum_{k=1}^{K} P_{s,k} T_{r,k} + P_{f,k} T_f \pi_k \leq E. \tag{$\widetilde{\text{C3.b}}$}$$

With the relaxation (7), ($\widetilde{\text{C2}}$), ($\widetilde{\text{C3.a}}$) and ($\widetilde{\text{C3.b}}$), the approximate optimal policy becomes

$$\begin{aligned} \underset{\boldsymbol{\pi}, \boldsymbol{P}_s}{\text{maximize}} \quad & \widehat{G}(\boldsymbol{\pi}, \boldsymbol{P}_s) \\ \text{subject to} \quad & \pi_k \in [0,1], \quad k \in \{1, \ldots, K\} \\ & P_{s,k} \in \mathbb{R}^+, \quad k \in \{1, \ldots, K\} \\ & \text{(C1) and } (\widetilde{\text{C2}}) \text{ and } (\widetilde{\text{C3.a}}) \text{ and } (\widetilde{\text{C3.b}}). \end{aligned} \tag{P1}$$

While the constraints of (P1) are linear, the optimization program (P1) is not convex, as the objective (7) to maximize is not a concave function. Yet, the program (P1) amounts to maximizing a sum of multiple fractional terms, often called the sum-of-ratios problem. In general, sum-of-ratios problems are NP-hard [22]. Fortunately, given the convex constraints and the concave-over-convex form of the ratios, the simplified problem can be solved with the Jong method [23], which harnesses a reparameterization of the problem into a parametric convex program, and enjoys convergence guarantees towards the global optimum of the problem (P1). Moreover, it is to date the most efficient method for problems of this form [24].

IV. Numerical Experiments

We implement the optimization program (P1) in MATLAB using the CVX software for disciplined convex programming [25]. Two experiments are conducted to evaluate the proposed policy. First, our method is applied to a synthetic Gaussian mixture dataset; then, on a FMCW radar simulation dataset generated using MATLAB radar toolbox. The approximate optimal policy (P1) is compared against the *fair-sensing* and *importance-aware* policies. The fair sensing policy balances the sensing task for all devices, *i.e.* $\pi_1 = \pi_2 = \cdots = \pi_K$. The importance-aware scheme prioritizes the devices with higher discriminant gains by forcing $\pi_k = 1$ to the most discriminative devices until the constraints are violated, and $\pi_k = 0$ to the less discriminative devices.

For all experiments, we set the communication bandwidth $B = 10$ MHz around the carrier frequency 3.5 GHz, the durations of stages are $T_s = 2$s, $T_f = 0.1$s, and $T_{stall} = 4$s. The eMBB throughput guarantees (C2) are selected by letting SINR_k be the SINR level of the k-th device, which is quantized SINR_k^{std} using a grid of $\{-5, 0, ..., 35\}$ dB. Without sensing, the standard guarantee rate is $r_k^{std} = e_k^{std} B/K$, where the spectral efficiency e_k^{std} is computed from SINR_k^{std}. The guarantee rate is computed as

$$r_k^{min} = \gamma r_k^{std}, \quad k \in \{1, \cdots, K\}, \tag{9}$$

where γ represents the *guarantee level* common to all devices.

A. Classification of a Synthetic Gaussian Dataset

In this experiment, we consider $L = 2$ classes, an ensemble of $K = 20$ devices, and $N = 10$ features per device. It is further assumed $\boldsymbol{\Sigma}_k = \boldsymbol{I}_N$ and $\sigma_r^2 = 1$. The devices are located randomly in a crown of inner radius 100m and outer radius 1000m centered at the fusion center. The transmitted power is subject to the path loss and shadowing, leading to the received power:

$$P_{rx} = P_{tx} - \beta - 10\alpha \log_{10}(d) - \psi, \tag{10}$$

where α is the path loss exponent, d is the distance between the sender and receiver, β is the constant path loss component and $\psi \sim \mathcal{N}(0, \sigma_\psi^2)$ is the shadowing. The SINR is then computed by introducing a noise of spectral density -174dBm/Hz, and interference is modeled by a noise rise of 6dB. We consider five categories of devices with transmitting powers

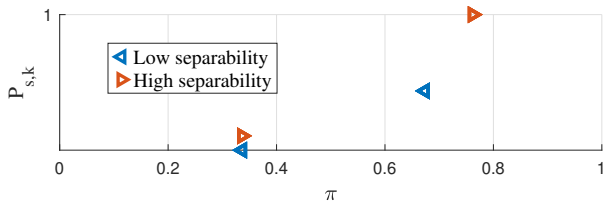

Figure 2: Illustration of optimal policy (P1) for two different separation between the class centers. In the setting of the simulations, each marker corresponds to 5 devices.

of $0.1, 0.2, 0.4, 0.6$, and 1W. The maximum allowed sensing power $P_{\max,k}$ is selected twice as that of the transmitting power of the device. The energy constraint is set to 80% of the maximum value (when all devices are scheduled to sense at maximum power in every cycle).

We start the simulation by assessing the effect of the separability between the classes on the optimal policy (P1). Herein, 20 devices are divided into two groups depending on the levels of separability, defined as the distance between the class centers $\mu_{k,1} - \mu_{k,2}$. Figure 2 pictures the policies applied to the devices as a function of the separability perceived by the sensors. It can be appreciated that the optimal policy prioritizes devices with high separability. We note that some devices, which have $\pi_k > 0$ and $P_{s,k} = 0$, do not sense or send eMBB data in the sensing stage in order to save energy and dedicate bandwidth to others.

We now move to the complete simulation setting, where devices are drawn randomly in the considered zone, and the class center The class are drawn such that $(\mu_{k,1} - \mu_{k,2}) \sim \mathcal{N}(0, \boldsymbol{I}_N)$. Figure 3a shows the sensing benefit of our scheduling policy compared to the fair sensing and importance-aware policies. The gap between the discriminant gain of the optimal policy and the other two increases with higher values of the data service guarantee level γ until $\gamma \simeq 1.1$. The gain rapidly decreases above that threshold as sensing is impossible without sacrificing the mean eMBB performance. Figure 3b showcases that, despite the improved sensing capability of the optimal policy, the sensing devices do not have to significantly compromise their eMBB data rate to jointly perform sensing under an appropriate policy.

B. Classification of Human Motions from Radar Samples

Inspired by [8], we adapt our framework to classify child walking, child pacing, adult walking, and adult pacing patterns from FMCW signals. Unlike [8], where a primitive-based autoregressive hybrid channel model (PBAH) was employed, we fully utilize the radar signal simulated by a MATLAB toolbox at four carrier frequencies: 5GHz, 12GHz, 24GHz, and 79GHz, while the sensing bandwidth is 10MHz for all bands. The heights of children and adults are uniformly distributed in the range $[0.9m, 1.2m]$ and $[1.5m, 2m]$, respectively. The speeds of walking and pacing are $0.5H$m/s and $0.25H$m/s, where H is the human height. The heading of moving humans is uniformly distributed in the $[-180, 180]$ degrees interval.

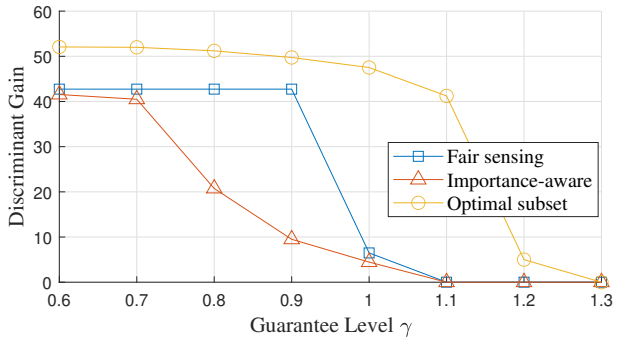

(a) Theoretical discriminant gain against the guarantee level γ.

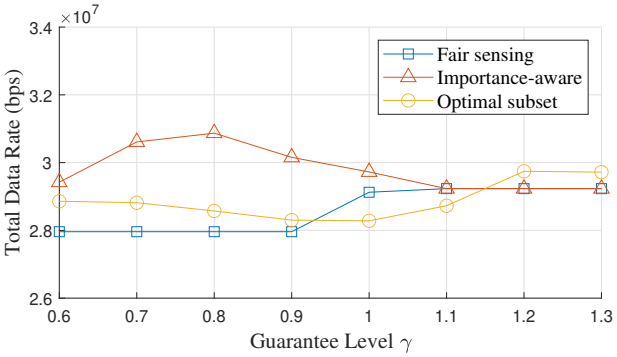

(b) Total eMBB rate against the guarantee level γ.

Figure 3: Sensing and communication performance against the guarantee level γ on synthetic Gaussian data.

The sensing area is 20 meters wide by 40 meters long in front of the sensing device. A dataset consisting of 800 training samples and 200 testing samples is created for each band. The samples are distributed uniformly over the classes, while the fusion center trains a support vector machine (SVM) model for classifying the human motions sensed by the devices.

We randomly distribute $K = 20$ devices in 15 regions and extract the $N_k = 100$ leading PCA features of the device samples. The data distributions $p_{k,\ell}$ are approximated by Gaussians with the same sample means and covariances. A sensing power of 2W corresponding to an SNR level of 20dB is selected. The communication distance and energy constraint are the same as those in the first experiment, and the sensing band is chosen randomly from the four values. The classification results are pictured in Figure 4. It is interesting that the accuracies of predictions by SVM follow the same trend as that of the theoretical gain, even though the network classification objective relies on many modeling approximations. This suggests the robustness of the proposed scheme and its practical application potential. When the discriminant gain falls to 0, the fusion center accuracy is about 25%, corresponding to that of a random guess.

V. CONCLUSION

In this paper, we presented a scalable goal-oriented framework for ISAC, integrating the global vision of the system,

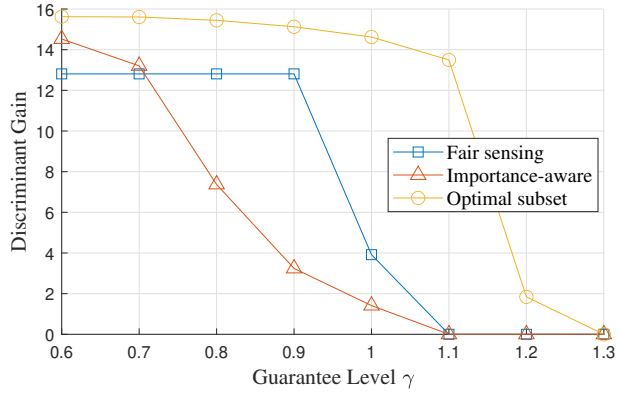

(a) Theoretical discriminant gain against the guarantee level γ.

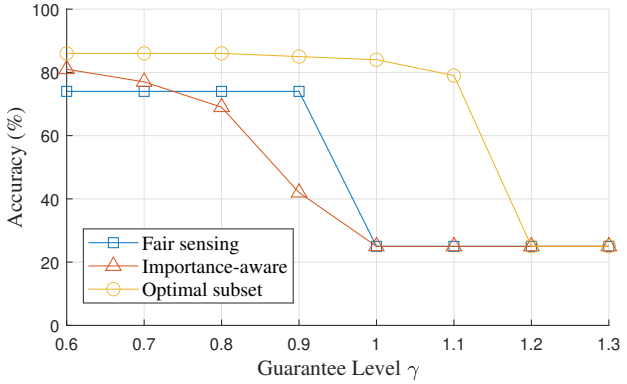

(b) Accuracy of the fusion center classification with an SVM against the guarantee level γ.

Figure 4: Classification performance with MATLAB FMCW radar simulation data, $K = 20$ devices monitoring 15 regions.

including the performance of the eMBB service as well as the resource, device power, and total system energy constraints. The goal towards optimization is the sensing accuracy through the concept of discriminant gain. We formulated an associated constrained optimization problem and obtained the optimal policy through computationally tractable relaxations. Experiments with a perfect and imperfect Gaussian mixture prior demonstrated the benefits of the proposed scheme. Future works will consider the balancing precision of predictions between classes, the freshness of states of sensing areas, and more precise modeling of the goal application.

References

[1] F. Liu, Y. Cui, C. Masouros, J. Xu, T. X. Han, Y. C. Eldar, and S. Buzzi, "Integrated sensing and communications: Toward dual-functional wireless networks for 6G and beyond," *IEEE journal on selected areas in communications*, vol. 40, no. 6, pp. 1728–1767, 2022.

[2] X. Zhu, J. Liu, L. Lu, T. Zhang, T. Qiu, C. Wang, and Y. Liu, "Enabling intelligent connectivity: A survey of secure isac in 6g networks," *IEEE Communications Surveys & Tutorials*, 2024.

[3] A. Liu, Z. Huang, M. Li, Y. Wan, W. Li, T. X. Han, C. Liu, R. Du, D. K. P. Tan, J. Lu *et al.*, "A survey on fundamental limits of integrated sensing and communication," *IEEE Communications Surveys & Tutorials*, vol. 24, no. 2, pp. 994–1034, 2022.

[4] B. K. Chalise, M. G. Amin, and B. Himed, "Performance tradeoff in a unified passive radar and communications system," *IEEE Signal Processing Letters*, vol. 24, no. 9, pp. 1275–1279, 2017.

[5] F. Liu, Y.-F. Liu, A. Li, C. Masouros, and Y. C. Eldar, "Cramér-rao bound optimization for joint radar-communication beamforming," *IEEE Transactions on Signal Processing*, vol. 70, pp. 240–253, 2021.

[6] J. Guerci, R. Guerci, A. Lackpour, and D. Moskowitz, "Joint design and operation of shared spectrum access for radar and communications," in *2015 IEEE Radar Conference (RadarCon)*. IEEE, 2015, pp. 0761–0766.

[7] G. Li, S. Wang, J. Li, R. Wang, F. Liu, X. Peng, T. X. Han, and C. Xu, "Integrated sensing and communication from learning perspective: An sdp3 approach," *IEEE Internet of Things Journal*, vol. 11, no. 4, pp. 5589–5603, 2023.

[8] D. Wen, P. Liu, G. Zhu, Y. Shi, J. Xu, Y. C. Eldar, and S. Cui, "Task-oriented sensing, computation, and communication integration for multi-device edge ai," *IEEE Transactions on Wireless Communications*, vol. 23, no. 3, pp. 2486–2502, 2023.

[9] M. Ferreira Da Costa, S. E. Elayoubi, and W. Hajji, "Goal-oriented communications for distributed sensing: a joint scheduling and estimation approach," in *IEEE VTC-Spring*, 2024.

[10] K. Meng, C. Masouros, A. P. Petropulu, and L. Hanzo, "Cooperative isac networks: Opportunities and challenges," *IEEE Wireless Communications*, pp. 1–8, 2024.

[11] E. C. Strinati and S. Barbarossa, "6G networks: Beyond shannon towards semantic and goal-oriented communications," *Computer Networks*, vol. 190, p. 107930, 2021.

[12] T. M. Getu, G. Kaddoum, and M. Bennis, "A survey on goal-oriented semantic communication: Techniques, challenges, and future directions," *IEEE Access*, 2024.

[13] D. Gündüz, Z. Qin, I. E. Aguerri, H. S. Dhillon, Z. Yang, A. Yener, K. K. Wong, and C.-B. Chae, "Beyond transmitting bits: Context, semantics, and task-oriented communications," *IEEE Journal on Selected Areas in Communications*, vol. 41, no. 1, pp. 5–41, 2022.

[14] S. E. Elayoubi and E. Hardouin, "For an energy sober network that contributes to a sustainable society," in *2023 IEEE Future Networks World Forum (FNWF)*. IEEE, 2023, pp. 1–7.

[15] Q. Lan, Q. Zeng, P. Popovski, D. Gündüz, and K. Huang, "Progressive feature transmission for split classification at the wireless edge," *IEEE Transactions on Wireless Communications*, vol. 22, no. 6, pp. 3837–3852, 2022.

[16] M. Series, "Imt vision–framework and overall objectives of the future development of imt for 2020 and beyond," *Recommendation ITU*, vol. 2083, pp. 1–21, 2015.

[17] F. Liu, L. Zhou, C. Masouros, A. Li, W. Luo, and A. Petropulu, "Toward dual-functional radar-communication systems: Optimal waveform design," *IEEE Transactions on Signal Processing*, vol. 66, no. 16, pp. 4264–4279, 2018.

[18] W. Hoeffding, "Asymptotically optimal tests for multinomial distributions," *The Annals of Mathematical Statistics*, pp. 369–401, 1965.

[19] M. Jovanovic, M. K. Karray, and B. Blaszczyszyn, "Qos and network performance estimation in heterogeneous cellular networks validated by real-field measurements," in *ACM symposium on Performance evaluation of wireless ad hoc, sensor, & ubiquitous networks*, 2014, pp. 25–32.

[20] J.-B. Landre, Z. El Rawas, and R. Visoz, "Lte performance assessment prediction versus field measurements," in *2013 IEEE 24th Annual International Symposium on Personal, Indoor, and Mobile Radio Communications (PIMRC)*. IEEE, 2013, pp. 2866–2870.

[21] G. P. McCormick, "Computability of global solutions to factorable nonconvex programs: Part i—convex underestimating problems," *Mathematical programming*, vol. 10, no. 1, pp. 147–175, 1976.

[22] R. W. Freund and F. Jarre, "Solving the Sum-of-Ratios problem by an Interior-Point method," *Journal of Global Optimization*, vol. 19, no. 1, pp. 83–102, Jan. 2001.

[23] Y.-C. Jong, "An efficient global optimization algorithm for nonlinear sum-of-ratios problem," *Optimization Online*, vol. 32, pp. 38–39, 2012.

[24] L. Qian, W. Yu, P. Si, and J. Zhao, "Applications of inequalities to optimization in communication networking: Novel decoupling techniques and bounds for multiplicative terms through successive convex approximation," *arXiv preprint arXiv:2412.05828*, 2024.

[25] M. Grant and S. Boyd, "Cvx: Matlab software for disciplined convex programming, version 2.1," 2014.